This article has been accepted for publication in IEEE Transactions on Magnetics. This is the author's version which has not been fully edited and content may change prior to final publication. Citation information: DOI 10.1109/TMAG.2025.3632479

Blind Efficient Method for Optimizing Jiles-Atherton Model Parameters

Juan Manuel Conde Garrido[1,2,a], Jone Ugarte Valdivielso[3,b], Jose I. Aizpurua[4,5,c], Manex Barrenetxea Iñarra[3,d] and Josefina María Silveyra[1,2,e]

[1] Universidad de Buenos Aires. Facultad de Ingeniería. Laboratorio de Sólidos Amorfos, Argentina
[2] CONICET - Universidad de Buenos Aires. Instituto de tecnologías y Ciencias de la ingeniería "Hilario Fernández Long" (INTECIN), Argentina
[3] Electronics and Computing Science Department, Mondragon Unibertsitatea, Arrasate 20500, Spain
[4] Computer Science and Artificial Intelligence Department, University of the Basque Country (UPV/EHU), Donostia-San Sebastian, 20018, Spain
[5] Ikerbasque, Basque Foundation for Science, Bilbao 48009, Spain
[a] jmcondegarrido@fi.uba.ar ORCID: 0000-0002-7689-3912
[b] jugarte@mondragon.edu ORCID: 0000-0002-0612-1722
[c] joxe.aizpurua@ehu.eus ORCID: 0000-0002-8653-6011
[d] mbarrenetxeai@mondragon.edu ORCID: 0000-0002-0577-0106
[e] jsilveyra@fi.uba.ar ORCID: 0000-0003-0307-3419

We introduce a novel blind optimization method for determining the parameters of the Jiles-Atherton model of hysteresis, eliminating the need for user-provided initial guesses or search spaces. A carefully designed initialization procedure combined with a standard optimizer yields a high-performing, practical method for parameter estimation. Validation against a theoretical benchmark recovers ground-truth parameters in under half a minute with negligible error (relative error < 4×10^{-8}). When applied to the TEAM32 electrical steel experimental benchmark, our method achieved superior accuracy than previously reported fittings, also converging in under half a minute. Consistently robust performance is further demonstrated across diverse systems, including soft ferrites, nanocrystalline alloys, and magnetostrictive compounds. The presented blind approach offers new insights into magnetic material characterization and is deployed as an automated tool for hysteresis analysis. It advances both fundamental understanding and practical applications by demonstrating the Jiles-Atherton model's capability to describe anisotropic materials and by revealing its inherent limitations.

***Index Terms*—Jiles-Atherton, optimization, hysteresis, ferromagnetic, ferroelectric, non-linear**

I. INTRODUCTION

In recent decades, significant efforts have been devoted to developing optimization techniques for determining the parameters of the Jiles-Atherton model, originally developed for describing rate-independent magnetic hysteresis and later adapted to ferroelectric hysteresis [1-3]. These efforts span a wide range of approaches, from brute-force search methods to metaheuristic algorithms. However, the no-free-lunch theorem [4, 5] asserts that, in the absence of prior assumptions about the problem, no optimization strategy can be universally superior to others [6]. This implies that while a metaheuristic algorithm may excel at fitting one type of hysteresis loop, it may perform poorly on others. Consequently, any prior knowledge that can guide the search process can and should be leveraged to improve both accuracy and efficiency. For instance, initializing parameters near known good values using Gaussian distributions has been shown to enhance the performance of metaheuristic algorithms compared to uniform initialization [7].

The challenge, however, lies in obtaining the right initial values and avoiding convergence to a local minimum. As most Jiles-Atherton model parameters are intrinsically unconstrained, defining the search space requires prior knowledge even for metaheuristic algorithms relying on uniform initialization or brute-force search methods. As a result, existing optimization approaches often require a time-consuming literature review to identify similar scenarios, followed by trial-and-error adjustments [8].

In this work, we propose a novel, fully automated strategy for determining the optimal Jiles-Atherton model parameters that describe a given symmetric hysteresis loop. The method functions as a blind tool, requiring no prior knowledge from the user. Although the computational time depends on the loop shape and on the hardware used, it typically completes within tens of seconds. The strategy comprises two key steps: (1) a systematic approach to estimate initial guesses for the five model parameters without any user assumptions, and (2) the application of the well-known derivative-free Nelder-Mead algorithm to minimize an objective function freely within an unconstrained search space. We demonstrate the effectiveness of this blind method by applying it to two benchmarking problems and by fitting hysteresis loops for various soft magnetic materials with widely varying magnetization and applied magnetic field ranges. Before delving into the optimization strategy, we present a systematic derivation and discussion of the evolution of the Jiles-Atherton model equations, aiming to clarify inconsistencies in the literature and ease the learning path for newcomers. We also analyze the numerical integration of the Jiles-Atherton differential equation, a frequently overlooked yet critical procedure that becomes particularly challenging in regions of steep susceptibility transitions; to address this, we identify a reliable approach validated through convergence studies.

This article has been accepted for publication in IEEE Transactions on Magnetics. This is the author's version which has not been fully edited and content may change prior to final publication. Citation information: DOI 10.1109/TMAG.2025.3632479

II. THE JILES-ATHERTON MODEL

In 1983, D. C. Jiles and D. L. Atherton proposed a model based on a mean-field approximation to describe both the initial magnetization curve and quasistatic hysteresis loops of ferromagnetic materials [9]. Its widespread adoption is largely due to the model's balance between a relatively simple equation of state and a solid theoretical foundation, although it has also faced criticism for certain physical assumptions and its treatment of energy balance [10-13]. Despite these concerns, the model remains popular for its ability to characterize ferromagnetic and ferroelectric materials with sufficient accuracy.

The backbone of the Jiles-Atherton model is the anhysteretic magnetization, "which represents a global energy minimum towards which the magnetization strives but is prevented from reaching because of impedances to domain wall motion" [14]. The anhysteretic magnetization along the direction of the applied field is typically described by the Langevin function as

$$M_{anh} = M_S \mathcal{L}\left(\frac{H_{eff}}{a}\right), \tag{1}$$

where M_S is the saturation magnetization, $\mathcal{L}(h) = \coth(h) - 1/h$ is the Langevin function, H_{eff} is the effective mean magnetic field, and $a = Nk_BT/(\mu_0 M_S)$, with N being the number of magnetic entities per unit volume, k_B the Boltzmann constant, T the absolute temperature, and μ_0 the vacuum magnetic permeability.

The concept of effective field was introduced by Weiss in 1907 to explain that the field acting on the elementary magnetic moments of a ferromagnetic system is not solely the external field H [15]. Instead, it is augmented by a uniform internal field, analogous to the internal pressure suggested by Van der Waals in fluid behavior modeling [16]. Weiss termed this internal field the molecular field and proposed that it is directly proportional to the sample's average magnetization M (average magnetic moment per unit volume),

$$H_{eff} = H + \alpha M, \tag{2}$$

where α is the molecular field constant, independent of temperature.

Jiles and Atherton adopted this mean-field parameter to explain magnetic ordering due to the quantum mechanical exchange interaction [17], and it is positive in ferromagnetic materials [18]. Silveyra and Conde Garrido recently extended this theory, suggesting that the internal field αM can either aid or oppose the external field H in ferromagnetic materials [19]. They proposed that α depends on crystal electric forces that align the elementary effective magnetic moments to minimize the crystal field and spin-orbit energies [20]. This extension allows the Langevin-Weiss approach to describe materials beyond those with low anisotropy, as originally explained by Jiles [21].

Combining Eqs. (1) and (2), the anhysteretic magnetization is expressed as

$$M_{anh} = M_S \mathcal{L}\left(\frac{H + \alpha M}{a}\right). \tag{3}$$

This expression, originally formulated by Jiles and Atherton in 1983 [9], remains the standard representation for anhysteretic magnetization in their model, despite some criticism. Since the material's magnetization M is hysteretic, Eq. (3) implies that the anhysteretic magnetization is also hysteretic. To address this, an alternative formulation has been proposed, where the internal field is αM_{anh} rather than αM [22],

$$M_{anh} = M_S \mathcal{L}\left(\frac{H + \alpha M_{anh}}{a}\right). \tag{4}$$

However, in this work, we adhere to Eq. (3) due to its widespread adoption.

The Jiles-Atherton model (from 1989 onward [14]) states that the magnetization of the material M is related to the anhysteretic magnetization [Eq. (3)] and an irreversible magnetization M_{irr} through the reversibility factor c, which ranges from 0 to 1,

$$M = cM_{anh} + (1 - c)M_{irr}. \tag{5}$$

Instead of this weighed sum, an alternative yet equivalent formulation often reported expresses the magnetization as the sum of the irreversible magnetization and a reversible magnetization defined as $M_{rev} = c(M_{anh} - M_{irr})$ [14].

Jiles and Atherton conceptualized ferromagnetic hysteresis through an energy-based framework, attributing the phenomenon to pinning effects at magnetic inhomogeneities that resist changes in the irreversible magnetization. Their model originated from an energy-balance analysis of complete hysteresis cycles in the $M - H$ plane, quantifying energy dissipation as arising from a friction-like force. They then extended this formulation to apply it to partial (non-closed) trajectories of the hysteresis loop leading to the differential equation

$$M_{irr} = M_{anh} - \delta k \frac{dM_{irr}}{dH_{eff}}, \tag{6}$$

where k represents the pinning factor quantifying the strength of the friction-like loss mechanism, and $\delta = \text{sign}(dH)$ is a directional parameter ensuring that pinning always opposes magnetization changes, thereby maintaining energy dissipation [23]. The pinning factor k directly influences the separation between the initial magnetization curve and the anhysteretic curve, where increasing values of k lead to progressively greater displacement between them [14]. Initially treated as a constant [9], later studies suggested k may vary with both M and H [18, 23]. Among the various formulations proposed by Jiles and collaborators to describe the friction-like process [9, 22-25], we employ Eq. (6) with k being constant due to its widespread adoption.

Removing intermediate variables to solve the magnetization easily (see Appendix A) yields the following first-order ordinary differential equation,

$$\frac{dM}{dH} = \frac{k\delta c \frac{dM_{anh}}{dH_{eff}} + (M_{anh} - M)\delta_M}{k\delta - \alpha\left[k\delta c \frac{dM_{anh}}{dH_{eff}} + (M_{anh} - M)\delta_M\right]}, \tag{7}$$

where the anhysteretic magnetization and its derivative with respect to the effective field are given by

$$M_{anh} = M_S \mathcal{L}\left(\frac{H + \alpha M}{a}\right) = \\ = M_S\left[\coth\left(\frac{H + \alpha M}{a}\right) - \frac{1}{H + \alpha M}\right], \tag{8}$$

and

$$\frac{dM_{anh}}{dH_{eff}} = \frac{M_S}{a}\mathcal{L}'\left(\frac{H+\alpha M}{a}\right) = \\ = \frac{M_S}{a}\left[-\operatorname{csch}^2\left(\frac{H+\alpha M}{a}\right) + \left(\frac{a}{H+\alpha M}\right)^2\right]. \quad (9)$$

To avoid catastrophic cancellation for small argument values, $\mathcal{L}(h)$ and $\mathcal{L}'(h)$ can be approximated by their Taylor expansion about the origin,

$$\mathcal{L}(h) \cong \frac{h}{3} - \frac{1}{45}h^3 + \frac{2}{945}h^5, \quad (10)$$

$$\mathcal{L}'(h) \cong \frac{1}{3} - \frac{h^2}{15} + \frac{2}{189}h^4. \quad (11)$$

Lastly, the step function in Eq. (7),

$$\delta_M = \frac{1}{2}[1 + \operatorname{sgn}(M_{anh} - M)\delta], \quad (12)$$

is a patch preventing negative differential magnetic susceptibilities (which are generated by the unpatched model right after a turning point). Combined with an initial condition (typically the demagnetized state), Eq. (7) describes ferromagnets hysteretic magnetization. Appendix B outlines alternative rate-independent hysteresis formulations proposed by Jiles and collaborators, with the aim of helping readers understand the varying results reported in the literature. Moreover, by clarifying the origins of each equation, readers can more easily adapt our optimization method to other model variants if needed.

III. NUMERICAL SOLUTION OF THE ORDINARY DIFFERENTIAL EQUATION

Since the Jiles-Atherton ordinary differential equation [Eq. (7)] has no analytical solution, it must be solved using numerical integration methods. Accurate integration is particularly critical in regions with steep susceptibility transitions. In our experience, different numerical methods –even within the same optimization framework– can yield markedly different results. We therefore discuss common approaches used in the literature and describe in detail the numerical method that proved most reliable based on convergence studies we conducted as guidance to future users.

Both Euler [26] and Runge-Kutta [27] methods have been recommended in standard references to numerically solve the Jiles-Atherton ordinary differential equation. Between these two, the Runge-Kutta family offers substantial advantages over the basic Euler method. While Euler methods are simple and computationally economical, they may suffer from poor accuracy and numerical stability for stiff or highly nonlinear differential equations like the Jiles-Atherton model. In contrast, higher-order Runge-Kutta methods achieve significantly better accuracy without a proportional increase in computational cost, reducing truncation errors while maintaining stability.

Another improvement in numerical integration involves adaptive step-size control. Traditional fixed-step methods depend on user-defined step sizes, risking either excessive computation (from overly small steps) or compromised accuracy (from overly large steps) [28]. Adaptive methods dynamically adjust step sizes based on local error estimates, refining steps in rapidly changing regions and coarsening them in smoother intervals, independently of the step sizes of the experimental data.

The numerical stability of the solution can be further improved through careful configuration of tolerance parameters. Relative tolerance defines error proportionality across solution scales, while absolute tolerance establishes critical thresholds for significant solution variations –crucial for maintaining accuracy near zero-crossing regions.

In this work, we employed the TR-BDF2 method (MATLAB's `ode23tb` solver [29, 30]). This implicit Runge-Kutta pair of orders 2 and 3, uses adaptive step control and combines the trapezoidal rule with the backward differentiation formula of order 2 for the numerical integration of stiff ordinary equations. The solver was optimized with a relative tolerance of 1×10^{-7} and an absolute tolerance of 1×10^{-6} to ensure computational efficiency and accuracy.

IV. LIMITATIONS OF CURRENT PARAMETER OPTIMIZATION STRATEGIES FOR THE JILES-ATHERTON MODEL

Accurate parameter identification for the Jiles-Atherton model remains challenging due to fundamental limitations in existing optimization strategies. The model's implicit formulation results in a highly nonlinear inverse problem, where parameters exhibit significant sensitivity to minor variations in hysteresis loops [25].

The original fitting method developed by Jiles *et al.* [14, 25] –described as "the result of several years (of) work on modelling hysteresis"– poses impractical requirements: (1) availability of anhysteretic and initial magnetization curves, which are typically unavailable alongside standard hysteresis data, (2) prior knowledge of M_S, which is often unknown, with theoretical values sometimes leading to poor fits [31], (3) user-provided initial guesses of α, and (4) manual trial-and-error refinement [32, 33]. Although Jiles *et al.* reported accuracy "to within a few percent in most cases" [14], the method has demonstrated convergence issues under certain conditions [33].

Brute-force parameter searches [34] can be prohibitively slow, with reported cases requiring 20-167 minutes per loop [7], and they do not guarantee finding global optima [35]. Alternative strategies to improve search efficiency, such as heuristic strategies like coarse-to-fine searches [34] and deterministic global optimization methods like branch-and-bound [33], help mitigate but do not fully eliminate scalability challenges. Over the past two decades, advances in computational power have led to the widespread adoption of metaheuristics for optimizing the Jiles-Atherton model parameters, including Differential Evolution [36-41], Genetic Algorithms [42, 43], and Particle Swarm Optimization [44, 45], Simulated Annealing [46], along with Nature-inspired variants such as the Shuffled Frog-Leaping Algorithm [47, 48], and Levy Whale Optimization [49]. While these methods significantly reduce computational time compared to brute-force searches, they rely on artificially constrained parameter bounds (e.g., ± 100 % of reference values [45]), limiting their adaptability to unknown material systems. Even machine learning approaches [50, 51]

require pre-existing databases of solved cases to learn dynamics through supervised learning strategies, creating a circular dependency that limits applicability to real-world problems.

Ultimately, all current optimization methods assume some prior knowledge of plausible parameter ranges. In practice, users often lack even order-of-magnitude estimates, making these approaches impractical for novel materials or measurement conditions.

V. THE PROPOSED BLIND METHOD

We present a two-stage optimization strategy that systematically overcomes the limitations of existing approaches. The method consists of an automated parameter initialization procedure requiring no user input, followed by a derivative-free optimization algorithm, all while avoiding artificial constraints within the search space.

The initialization stage recognizes the distinct roles of the five model parameters: M_S, a, and α primarily shape the hysteresis loop's backbone, while k and c govern its width. The proposed approach builds upon the established similarity between the horizontal average curve of a symmetric hysteresis loop and the anhysteretic magnetization curve [52], the latter typically requiring specialized and time-consuming experimental procedures [53]. The recently developed MagAnalyst MATLAB toolbox [54] provides an efficient implementation for fitting these curves using the Langevin-Weiss equation of state [Eq. (4)]. While the standard Jiles-Atherton model defines the anhysteretic magnetization in terms of the hysteretic magnetization [Eq. (3)], both formulations yield similar curves. We exploit this similarity by using Eq. (4) to obtain, with the help of MagAnalyst, robust initial estimates for M_S, a, and α by fitting the horizontal average curve of a hysteresis loop in the $M-H$ plane. A key advantage of MagAnalyst is its ability to perform these fits without requiring predefined parameter ranges or initial guesses for neither M_S, a, nor α. Instead, it uses the tip of the data curve (i.e., the point measured at maximum external field) as a fixed reference and reparametrizes the search space through a coordinate transformation into two intrinsically bounded variables. User input can aid convergence for anhysteretic curves with multiple components [55], but this lies beyond the scope of the present work. This strategy, implemented in the MagAnalyst toolbox, has demonstrated robust performance across diverse material systems and challenged conventional assumptions about Weiss' constant α, with both positive and negative values now recognized as physically meaningful [19, 20] –a finding that is gaining broader acceptance [56, 57].

For the reversibility parameter c, we adopt a fixed initial estimate of 1/3, a value that consistently yields robust results across all materials and conditions tested.

To estimate k, we leverage the negative coercive point of the hysteresis loop as a fixed reference, though in principle, any other point could be used. The idea is to select the point farthest from the tip used in the first step. Solving Eq. (7) for k yields

$$k = \frac{(M_{anh} - M)}{-\delta\left[c\frac{dM_{anh}}{dH_{eff}} - \left(\frac{dM}{dH}^{-1} + \alpha\right)^{-1}\right]}. \quad (13)$$

At the coercive point on the descending branch of the loop, $\delta = -1$ and $M = 0$. The coercive field $H = -H_C$ is obtained via interpolation from the left branch, while the corresponding susceptibility $dM/dH = \chi_C$ is obtained by interpolating the numerical derivative of that branch. Then, we derive the closed-form expression for k

$$k = \frac{M_S \mathcal{L}\left(-\frac{H_C}{a}\right)}{c\frac{M_S}{a}\mathcal{L}'\left(-\frac{H_C}{a}\right) - (\chi_C{}^{-1} + \alpha)^{-1}}, \quad (14)$$

where M_S, a, α, and c use the estimates from previous steps. A similar approach could be considered for estimating k in alternative formulations of the model.

With all five parameters initialized, we applied a well-established optimization algorithm to refine the solution by minimizing an objective error function. To this end, we deliberately selected a simple, effective, and freely available routine based on the Nelder-Mead method: the `minimize` library [58]. Yet, this modular framework allows users to employ alternative algorithms, if desired. The objective error function is defined as a relative error, computed in the normalized $M-H$ plane. It represents the mean orthogonal distance [20] between (1) points uniformly distributed along the left branch of the experimental hysteresis loop (generated using MATLAB's `interparc` library [59] to ensure equal arclength spacing) and (2) the corresponding modeled curve. The modeled curve is constructed by numerically integrating the differential equation $M' = f(H, M)$ [Eq. (7)] using MATLAB's `ode23tb` library. The integration begins with a forward sweep from $H = 0$ to $H = H_{TIP}$, the maximum applied field, using the initial condition $M = 0$. While this first magnetization curve is not utilized for calculating the relative error, the resulting magnetization at $H = H_{TIP}$ serves as the initial condition for integrating from $H = H_{TIP}$ back to $H = -H_{TIP}$, yielding the modeled curve used to compute the relative error. The optimization routine is configured with a maximum of 10^3 iterations and 10^4 function evaluations, and termination tolerances of 10^{-4} for both the solution vector and the function value. Large penalties are imposed when parameters fall outside their intrinsic bounds ($a < 0$, $k < 0$, $c < 0$, and $c > 1$). The elapsed time is recorded for both the initial estimates calculation and the subsequent optimization stage, with the total computation time for the blind method being the sum of these two stages.

This method represents the first truly blind implementation for Jiles-Atherton parameter optimization, eliminating the need for expert knowledge or reference data, while preserving the physical interpretability of all model parameters. The following sections will demonstrate the robustness of this blind method across diverse materials.

TABLE I

JILES-ATHERTON MODEL PARAMETERS FOR VALIDATION USING A THEORETICAL MATERIAL. GROUND-TRUTH PARAMETERS USED TO GENERATE THE DATA CURVE, ALONG WITH THOSE RETRIEVED BY JILES ET AL. [25], CHWASTEK & SZCZYGŁOWSKI [33], AND THE BLIND METHOD, BOTH FROM THE PROPOSED INITIAL ESTIMATION STAGE AND THE FINAL OPTIMIZED SOLUTION.

Parameters	Data	Jiles et al.	Chwastek & Szczygłowski	Blind method: initial estimates	Blind method: optimized estimates
M_S(A/m)	1.7×10^{6}	1.7×10^{6} *	1.71×10^{6}	1.69×10^{6}	1.699996×10^{6}
a (A/m)	1000	1015	1119.6	934.7	999.998
α	1×10^{-3}	1.08×10^{-3}	1.2×10^{-3}	0.8×10^{-3}	0.99998×10^{-3}
c	0.1	0.102	0.296	0.333	0.0999
k (A/m)	500	490	644.9	631.3	499.93
Relative error	-	8.30×10^{-5}	2.00×10^{-4}	1.95×10^{-4}	3.81×10^{-8}
Elapsed time (s)	-	-	~3600	5	21

* M_S was not fitted in this study.

VI. RESULTS AND DISCUSSION

A. Validation study using a theoretical material

To evaluate the blind method performance, we applied the fundamental test proposed by Jiles et al. [25]: recovering the ground-truth generating parameters (M_S, a, α, k, and c) from a synthetic hysteresis loop. To allow direct comparison with prior approaches, we adopted the benchmark parameters used by Jiles et al. to test their proposed optimization strategy [25], which were later also used by Chwastek and Szczygłowski to test their implementation of the branch-and-bound method [33].

The results, summarized in Table I, demonstrate significant improvements in both accuracy and efficiency. Near-perfect parameter recovery is achieved, reducing relative error (as defined in Section V) from approximately 10^{-4} in previous studies to 10^{-8}. Compared to Chwastek and Szczygłowski's implementation, the combination of the substantial hardware advancements (AMD Athlon @ 1 GHz, 256 MB of RAM vs. Intel Core i9-9900K @ 3.60 GHz, 32 GB of RAM) and our improved optimization strategy accounts for the significant reduction in computational time (1 hour vs. 26 seconds). Moreover, the blind method operates as a fully automated system, requiring no prior knowledge or manual intervention. The high accuracy of the generated hysteresis loops –with both the initial estimates and the final optimized parameters (Fig. 1)– demonstrates the robustness of this two-stage approach, while the computation time of under half a minute underscores its practical utility for routine analysis.

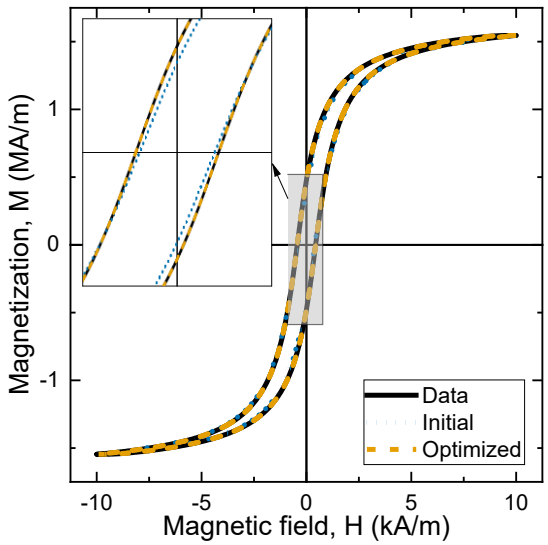

Fig. 1. Hysteresis loops of the validation study using a theoretical material generated with the ground-truth parameters (data), and those retrieved from the initial estimation stage (initial) and the optimization routine (optimized). All parameters are listed in Table I.

B. Validation study using real material data

To validate the blind method's practical performance, we applied it to a representative hysteresis loop from the TEAM32 benchmark dataset [60], whose measurement methodology is described therein. This dataset contains multiple loops measured for a commercial Fe-Si 3 wt.% non-oriented electrical steel (0.5 mm thickness); a material commonly used in rotating electrical machines. We selected a loop measured along the rolling direction, which had been previously fitted in the literature, allowing for direct comparison with previously retrieved parameters.

Table II compares the blind method's initial estimates and the optimized solution with the reference values reported by Hoffmann *et al.* [61]. Our results show strong agreement with the literature and achieve superior accuracy with computation times of under half a minute. Figure 2 shows the excellent agreement between the optimized modeled curve and the experimental data, confirming the effectiveness of the blind method for practical magnetic characterization.

TABLE II

JILES-ATHERTON MODEL PARAMETERS FOR VALIDATION USING REAL MATERIAL DATA (A NON-ORIENTED SILICON STEEL [60]). RETRIEVED PARAMETERS FROM HOFFMANN *ET AL.* [61] AND THE BLIND METHOD, OBTAINED THROUGH THE PROPOSED INITIAL ESTIMATION STAGE AND THE FINAL OPTIMIZED SOLUTION.

Parameters	Hoffmann *et al.*	Blind method: initial estimates	Blind method: optimized estimates
M_S(A/m)	1.33×10^{6}	1.29×10^{6}	1.32×10^{6}
a (A/m)	172.85	117.5	151.7
α	4.17×10^{-4}	2.33×10^{-4}	3.61×10^{-4}
c	0.652	0.333	0.572
k (A/m)	232.652	89.7	200.3
Relative error	7.76×10^{-4}	1.14×10^{-3}	3.46×10^{-4}
Elapsed time (s)	-	11	12

This article has been accepted for publication in IEEE Transactions on Magnetics. This is the author's version which has not been fully edited and content may change prior to final publication. Citation information: DOI 10.1109/TMAG.2025.3632479

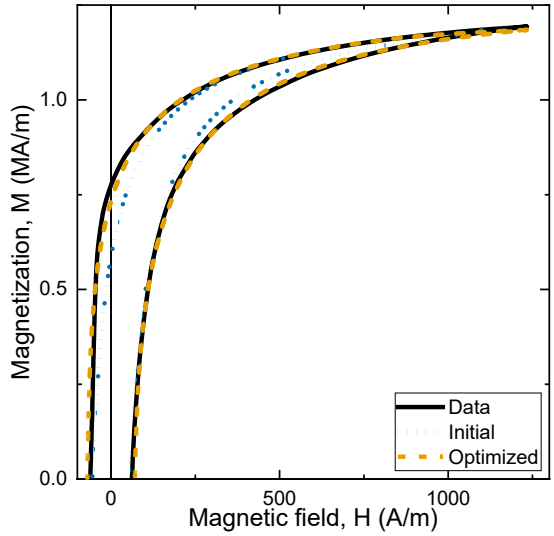

Fig. 2. Hysteresis loops of the validation study using real material data (a non-oriented silicon steel [60]). Modeled curves were generated using the retrieved parameters from the initial estimation stage (initial) and the optimization routine (optimized). The corresponding parameters are listed in Table II.

C. Validation across diverse magnetic materials

To rigorously evaluate the general applicability of the proposed method, we tested its performance across four distinct classes of soft magnetic materials, chosen to represent different magnetic behaviors and measurement conditions. The test set included: a soft Mn-Zn ferrite [62], a Fe-Cu-B nanocrystalline alloy with longitudinal anisotropy [63], a Fe-Cu-Nb-Si-B nanocrystalline alloy with transverse anisotropy [62], and a Terfenol-D magnetostrictive alloy [64], with measurement procedures detailed in the corresponding references. These materials exhibit a wide range of magnetizations and applied magnetic fields, providing a comprehensive validation of the approach.

The complete numerical results, including retrieved parameters, relative errors, and computation times, are presented in Table III. Visual comparison of experimental and modeled hysteresis loops in Figure 3 shows consistent accuracy across all material systems.

Several important conclusions emerge from these results. First, the two-stage blind method proved both effective and efficient across all analyzed cases, with even initial estimates showing sufficient accuracy for many practical applications. Proper tuning of the numerical integration solver was crucial for describing curves with strong nonlinearities, such as those in Fig. 3(b) and (c). The results also provide valuable insights into the capabilities and limitations of the Jiles-Atherton model itself. The model demonstrates notable versatility, successfully describing a wide range of magnetic systems, ranging from isotropic to anisotropic materials, measured both parallel and perpendicular to their easy axes. This finding challenges the original assumption by Jiles and Atherton that the model is only valid for isotropic ferromagnets with sigmoid-shaped curves when the anhysteretic magnetization is described by the Langevin function [21, 24]. Nonetheless, the discrepancies observed between modeled and experimental curves in Figure 3 reveal inherent limitations of the model rather than deficiencies in the optimization method. For instance, the Langevin function neglects possible magnetic inhomogeneities and mixed anisotropies within the material.

The comprehensive validation demonstrates that the proposed blind method is both robust and computationally efficient, with all cases converging in under half a minute across a wide range of magnetic materials. It also provides new insights into the fundamental capabilities and limitations of the Jiles-Atherton model. Moreover, the parameters optimized using this strategy can be applied not only in direct implementations of the model but also in inverse formulations suited for time-stepping finite-element simulations, provided the same set of underlying equations [Eqs. (1), (2), (3), (5), (6)] is used (see, e.g., [65]].

VII. CONCLUSION

This work addresses a longstanding challenge in Jiles-Atherton modeling by introducing a fully automated parameter optimization method that requires no prior knowledge or manual intervention. The core innovation lies in the combination of physics-guided initialization with numerical optimization, free from artificial constraints.

By recognizing the similarity between the horizontal average of the hysteresis loop and the anhysteretic magnetization curve, we derive accurate initial estimates for the parameters M_s, a, and α using a recently developed open-source toolbox. Setting c at 1/3 provides a robust default that yields consistent performance across a wide range of materials, while the coercive point enables a closed-form estimate for k. The final refinement step, performed without imposing artificial parameter bounds, overcomes a key limitation of previous approaches –namely, their reliance on

TABLE III
JILES-ATHERTON MODEL PARAMETERS RETRIEVED FOR DIFFERENT MATERIALS' HYSTERESIS LOOPS (SEE FIG. 3), INCLUDING BOTH THE INITIAL ESTIMATES AND THE OPTIMIZED PARAMETERS.

	Soft ferrite		Nanocrystalline alloy with longitudinal anisotropy		Nanocrystalline alloy with transverse anisotropy		Terfenol-D	
Parameters	**Initial**	**Optimized**	**Initial**	**Optimized**	**Initial**	**Optimized**	**Initial**	**Optimized**
M_S(A/m)	2.96×10^{5}	2.97×10^{5}	1.23×10^{6}	1.26×10^{6}	1.05×10^{6}	1.05×10^{6}	3.14×10^{5}	1.00×10^{6}
a (A/m)	16.3	15.53	3.67	5.29	2.11	2.25	954	51078
α	1.03×10^{-4}	9.22×10^{-5}	7.56×10^{-6}	1.50×10^{-5}	-2.09×10^{-4}	-2.08×10^{-4}	-2.94×10^{-2}	0.12
c	0.333	2×10^{-10}	0.333	7×10^{-5}	0.333	4×10^{-10}	0.333	0.779
k (A/m)	7.34	6.14	7.03	8.25	1.85	1.18	1802	7577
Relative error	1.57×10^{-3}	1.44×10^{-3}	4.72×10^{-3}	1.72×10^{-3}	9.82×10^{-5}	8.83×10^{-5}	7.88×10^{-3}	9.56×10^{-4}
Elapsed time (s)	5	7	0.05	21	5	15	3	12

This article has been accepted for publication in IEEE Transactions on Magnetics. This is the author's version which has not been fully edited and content may change prior to final publication. Citation information: DOI 10.1109/TMAG.2025.3632479

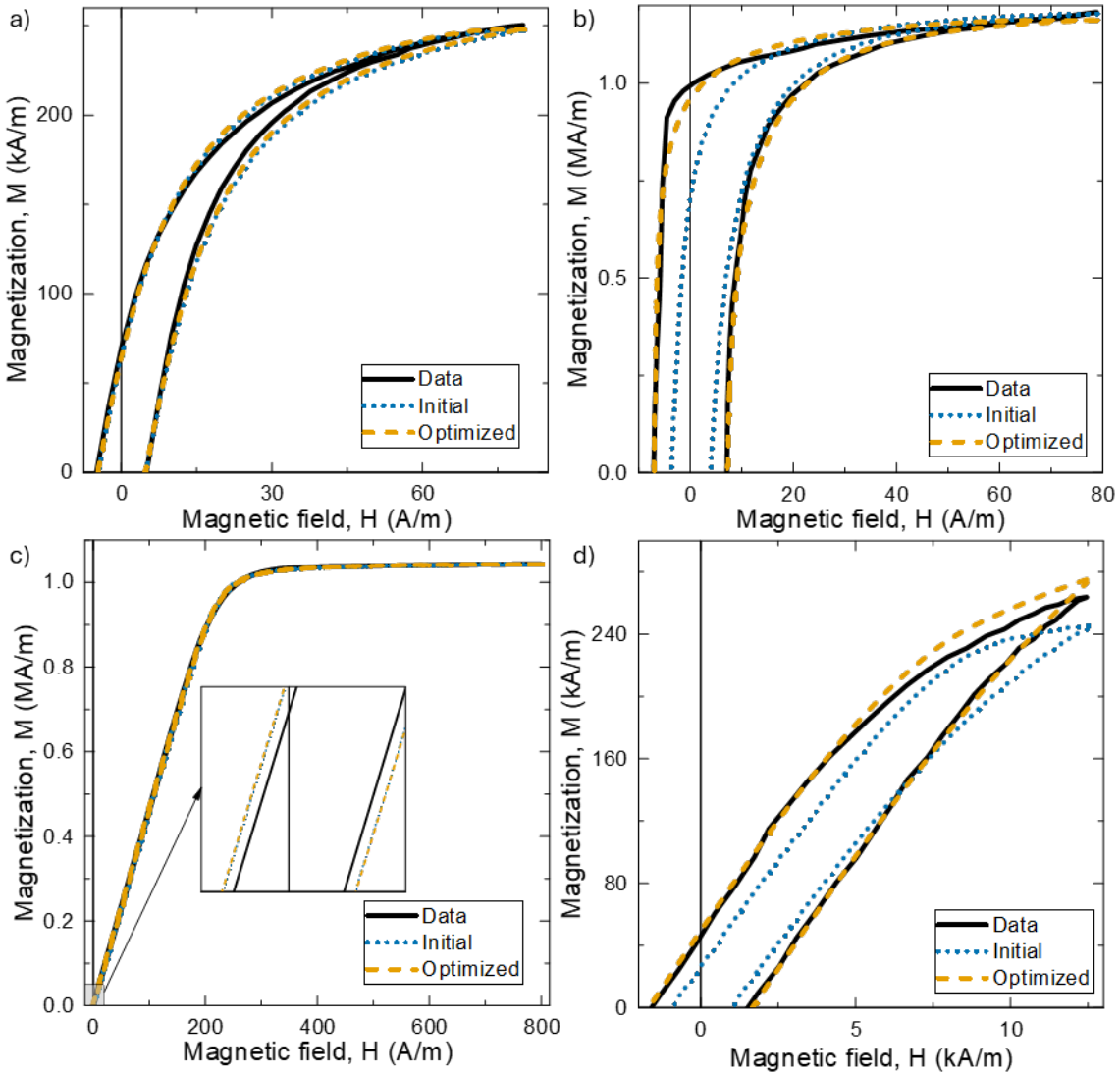

Fig. 3. Hysteresis loops of different of soft magnetic materials: (a) a soft Mn-Zn ferrite [62], (b) a Fe-Cu-B nanocrystalline alloy with longitudinal anisotropy [63], (c) a Fe-Cu-Nb-Si-B nanocrystalline alloy with transverse anisotropy [62], and (d) a Terfenol-D magnetostrictive alloy [64]. Modeled curves were generated with the retrieved parameters from the initial estimation stage (initial) and the optimization routine (optimized). The corresponding sets of parameters are listed in Table III.

case-specific tuning or manual constraints that hinder reproducibility and broader adoption of the Jiles-Atherton model.

The effectiveness and efficiency of the blind method are demonstrated through rigorous validation. For the theoretical benchmark, it recovered ground-truth parameters with near-perfect accuracy in under half a minute, distinctly outperforming reported implementations. Given its proven versatility across diverse magnetic materials –electrical steels, soft ferrites, nanocrystalline alloys, and magnetostrictive compounds– the same strategy shows promise for extension to hysteresis modeling in ferroelectric materials.

Beyond performance, our results also challenge the conventional assumption that the Langevin-based Jiles-Atherton model is restricted to isotropic systems. Successful fits of materials with induced uniaxial anisotropy, measured parallel and transversally to their easy axes, suggest broader applicability than previously recognized and support the idea that negative α values can yield physical meaningful descriptions. Remaining discrepancies –such as the varying relative errors across different examples– do not indicate a failure of the optimization method but rather reveal inherent limitations of the model itself. One such limitation is its single-component description of the anhysteretic magnetization, which may be insufficient for nonhomogeneous materials [20]. Moreover, the problem of accurately modeling *all* hysteresis loops –including minor loops, rate-dependent responses, or thermally activated effects– is fundamentally distinct from the parameter identification problem and lies beyond the scope of the standard Jiles-Atherton formulation. Nevertheless, the robust technique presented here for optimizing the model's five standard parameters may contribute to ongoing efforts aimed at extending the framework to describe a broader range of magnetization behaviors.

From a practical standpoint, this work significantly improves the accessibility and scalability of the Jiles-Atherton model. The proposed method eliminates the need for manual tuning and supports automated analysis of large

datasets, making it a valuable tool for both researchers and engineers.

ACKNOWLEDGMENT

J.M.C.G. and J.M.S. are funded by CONICET, Universidad de Buenos Aires (grant number UBACyT 20020190200001BA), and ANPCyT (grant number PICT-2019-2019-02122). J.U.V. and M.B.I. are funded by the Spanish State Research Agency (grant number CPP2021-008580) and the Department of Education of the Basque Government, Research Group Program (grant number IT1634-22). J. I. A. is funded by the Ramón y Cajal Fellowship, the Spanish State Research Agency (grant number RYC2022-037300-I), MCIU/AEI/10.13039/501100011033 and FSE+, and the Department of Education of the Basque Government, Research Group Program (grant number IT1504-22).

APPENDIX A: DERIVATION OF THE JILES-ATHERTON'S MODEL MAIN ORDINARY DIFFERENTIAL EQUATION

In this section, we derive the differential magnetic susceptibility which states the main ordinary differential equation of the most popular version of the Jiles-Atherton model [Eq. (7)], which has been employed throughout this work.

We begin with the model's definition of the effective magnetic field [Eq. (2)],

$$H_{eff} = H + \alpha M, \tag{A1}$$

where α is Weiss' molecular field constant. Differentiating this equation with respect to the applied magnetic field, H, yields

$$\frac{dH_{eff}}{dH} = 1 + \alpha \frac{dM}{dH}, \tag{A2}$$

The magnetic susceptibility, dM/dH, is obtained using the chain rule as

$$\frac{dM}{dH} = \frac{dM}{dH_{eff}} \frac{dHeff}{dH}. \tag{A3}$$

Substituting Eq. (A2) into Eq. (A3) and rearranging for dM/dH gives

$$\frac{dM}{dH} = \frac{dM}{dH_{eff}}\left(1 + \alpha \frac{dM}{dH}\right),$$
$$\frac{dM}{dH} = \frac{dM}{dH_{eff}} + \alpha \frac{dM}{dH_{eff}} \frac{dM}{dH},$$
$$\frac{dM}{dH}\left(1 - \alpha \frac{dM}{dH}\right) = \frac{dM}{dH_{eff}},$$
$$\frac{dM}{dH} = \frac{\frac{dM}{dH_{eff}}}{1 - \alpha \frac{dM}{dH_{eff}}}. \tag{A4}$$

Jiles and Atherton postulated that the magnetization, M, can be expressed as a weighed sum of the anhysteretic magnetization, M_{anh}, and the irreversible magnetization, M_{irr}, [Eq. (5)]

$$M = cM_{anh} + (1 - c)M_{irr}, \tag{A5}$$

with c being called the reversibility factor. This consideration was meant to allow domain walls in motion to be not necessarily planar and rigid but capable of bending. Differentiating Eq. (A5) with respect to H_{eff} gives

$$\frac{dM}{dH_{eff}} = c \frac{dM_{anh}}{dH_{eff}} + (1 - c) \frac{dM_{irr}}{dH_{eff}}. \tag{A6}$$

Substituting Eq. (A6) into Eq. (A4) yields

$$\frac{dM}{dH} = \frac{c \frac{dM_{anh}}{dH_{eff}} + (1 - c) \frac{dM_{irr}}{dH_{eff}}}{1 - \alpha c \frac{dM_{anh}}{dH_{eff}} - \alpha(1 - c) \frac{dM_{irr}}{dH_{eff}}}, \tag{A7}$$

which is a formulation frequently found in the literature [26].

The irreversible magnetization is modeled as a friction-like process [Eq. (6)]

$$M_{irr} = M_{anh} - k\delta \frac{dM_{irr}}{dH_{eff}}, \tag{A8}$$

where k is the pinning factor and $\delta = \text{sign}(dH)$ is a directional parameter that takes a value of +1 when H increases from one step to the next, and -1 when it decreases. Substituting Eq. (A8) in Eq. (A5) gives

$$M = cM_{anh} + (1 - c)\left(M_{anh} - k\delta \frac{dM_{irr}}{dH_{eff}}\right),$$
$$M = cM_{anh} + M_{anh} - cM_{anh} - (1 - c)k\delta \frac{dM_{irr}}{dH_{eff}},$$
$$k\delta(1 - c) \frac{dM_{irr}}{dH_{eff}} = M_{anh} - M. \tag{A9}$$

Multiplying Eq. (A6) by $k\delta$ gives

$$k\delta \frac{dM}{dH_{eff}} = k\delta c \frac{dM_{anh}}{dH_{eff}} + k\delta(1 - c) \frac{dM_{irr}}{dH_{eff}}, \tag{A10}$$

and by substituting Eq. (A9) into Eq. (A10) we obtain

$$k\delta \frac{dM}{dH_{eff}} = k\delta c \frac{dM_{anh}}{dH_{eff}} + (M_{anh} - M), \tag{A11}$$

For $k \neq 0$, the numerator and denominator of Eq. (A4) can be multiplied by $k\delta$,

$$\frac{dM}{dH} = \frac{k\delta \frac{dM}{dH_{eff}}}{k\delta - \alpha k\delta \frac{dM}{dH_{eff}}}. \tag{A12}$$

and, by substituting Eq. (A11) into Eq. (A12) we obtain

$$\frac{dM}{dH} = \frac{k\delta c \frac{dM_{anh}}{dH_{eff}} + (M_{anh} - M)}{k\delta - \alpha\left[k\delta c \frac{dM_{anh}}{dH_{eff}} + (M_{anh} - M)\right]}. \tag{A13}$$

Compared to Eqs. (A7) and (A12), Eq. (A13) removes intermediate variables, simplifying the calculation of M. However, it can produce unphysical negative differential magnetic susceptibilities during the field reduction from the loop tip. To address this, a step function, δ_M, is introduced so that $\frac{dM_{irr}}{dH} = 0$ when M_{irr} is below M_{anh} in the first quadrant, or above M_{anh} in the third quadrant of the $M - H$ plane [25, 66]. This modification results in Eq. (7), used in the literature [33, 67, 68],

$$\frac{dM}{dH} = \frac{k\delta c \frac{dM_{anh}}{dH_{eff}} + (M_{anh} - M)\delta_M}{k\delta - \alpha\left[k\delta c \frac{dM_{anh}}{dH_{eff}} + (M_{anh} - M)\delta_M\right]}. \tag{A14}$$

Typically, the anhysteretic magnetization is described by the Langevin function [Eq. (1)],

$$M_{anh} = M_S \mathcal{L}\left(\frac{H_{eff}}{a}\right), \quad (A15)$$

where M_S is the saturation magnetization, $\mathcal{L}(h) = \coth(h) - 1/h$ is the Langevin function, and a is related to the density of the magnetic entities. The first derivative of M_{anh} with respect to H_{eff} is

$$\frac{dM_{anh}}{dH_{eff}} = \frac{M_S}{a}\mathcal{L}'\left(\frac{H_{eff}}{a}\right), \quad (A16)$$

where $\mathcal{L}'(h) = -\operatorname{csch}^2(h) + 1/h^2 = 1 - \coth^2(h) - 1/h^2$ is the first derivative of the Langevin function. To avoid numerical instability at small argument values, Taylor expansions are used around $h = 0$ (e.g. $|h| \le 0.001$): $\mathcal{L}(h) \cong \frac{h}{3} - \frac{1}{45}h^3 + \frac{2}{945}h^5$ and $\mathcal{L}'(h) \cong \frac{1}{3} - \frac{1}{15}h^2 + \frac{2}{189}h^4$.

For $k = 0$, Eq. (A16) is undefined, but from Eq. (A9), we obtain

$$M = M_{anh}. \quad (A17)$$

From Eq. (A8) we also find that $M_{irr} = M_{anh}$. From Eq. (A17) we get

$$\frac{dM}{dH} = \frac{dM_{anh}}{dH}. \quad (A18)$$

Applying the chain rule of differentiation, and using Eq. (A2) we obtain

$$\frac{dM}{dH} = \frac{dM_{anh}}{dH_{eff}}\frac{dH_{eff}}{dH},$$
$$\frac{dM}{dH} = \frac{M_S}{a}\mathcal{L}'\left(\frac{H_{eff}}{a}\right)\left(1 + \alpha\frac{dM}{dH}\right), \quad (A19)$$

Isolating dM/dH from Eq. (A19) gives

$$\frac{dM}{dH} = \frac{\frac{M_S}{a}\mathcal{L}'\left(\frac{H_{eff}}{a}\right)}{1 - \alpha\frac{M_S}{a}\mathcal{L}'\left(\frac{H_{eff}}{a}\right)}. \quad (A20)$$

For $c = 1$, from Eq. (A5), we also obtain that $M = M_{anh}$ [Eq. (A17)] and, thus, dM/dH is also described by Eq. (A20).

APPENDIX B: ALTERNATIVE FORMULATIONS OF THE JILES-ATHERTON MODEL

Eq. (7) [equal to Eq. (A14) in Appendix A] represents the main ordinary differential equation of the most popular version of the Jiles-Atherton model. However, Jiles and his collaborators have explored other formulations for describing rate-independent magnetic hysteresis. The aim of this appendix is twofold: first, to help readers interpret the varying results reported in the literature, which often arise from subtle differences between model variants; and second, to provide the necessary context for adapting the proposed optimization strategy to these alternative formulations, should a different version be adopted.

In their early works [9, 18, 23], Jiles and Atherton proposed that the frictional force affected dM/dH_{eff} rather than dM_{irr}/dH_{eff} [Eq. (6), equal to Eq. (A8)] as

$$M = M_{anh} - k\delta\frac{dM}{dH_{eff}}, \quad (B1)$$

(Note: the directional parameter, δ, was not explicitly stated in [9]). Using the chain rule of differentiation,

$$\frac{dM}{dH_{eff}} = \frac{dM}{dH}\frac{dH}{dH_{eff}}, \quad (B2)$$

Eq. (B1) can be rearranged as

$$M = M_{anh} - \delta k\frac{dM}{dH}\frac{dH}{dH_{eff}},$$
$$\delta k\frac{dM}{dH}\frac{dH}{dH_{eff}} = M_{anh} - M,$$
$$\delta k\frac{dM}{dH} = (M_{anh} - M)\frac{dH_{eff}}{dH}. \quad (B3)$$

Substituting Eq. (A2) into Eq. (B1) and solving for dM/dH yields,

$$\delta k\frac{dM}{dH} = (M_{anh} - M)\left(1 + \alpha\frac{dM}{dH}\right),$$
$$\frac{dM}{dH} = \frac{M_{anh} - M}{\delta k - \alpha(M_{anh} - M)}. \quad (B4)$$

In 1986, Jiles and Atherton revised Eq. (B1), replacing M with M_{irr} [Eq. (6), equal to Eq. (A8)]

$$M_{irr} = M_{anh} - \delta k\frac{dM_{irr}}{dH_{eff}}. \quad (B5)$$

They also replaced M with M_{irr} in Eq. (B4), leading to

$$\frac{dM_{irr}}{dH} = \frac{M_{anh} - M_{irr}}{\delta k - \alpha(M_{anh} - M_{irr})}. \quad (B6)$$

This equation was used in subsequent works by Jiles, Atherton, and coworkers [14, 21, 25, 69-74]. It is important to note that, although not mentioned in the articles, deriving Eq. (B6) requires replacing M with M_{irr} in the effective field definition [Eq. (2), equal to Eq. (A1)] so that the following relation is used instead of Eq. (A2),

$$\frac{dH_{eff}}{dH} = 1 + \alpha\frac{dM_{irr}}{dH}. \quad (B7)$$

The original effective field definition continued to be used for computing M_{anh} [Eq. (3)].

The differential susceptibility can be obtained by taking the derivative of Eq. (5) [equal to Eq. (A5)] with respect to H,

$$\frac{dM}{dH} = c\frac{dM_{anh}}{dH} + (1 - c)\frac{dM_{irr}}{dH}. \quad (B8)$$

Substituting it in Eq. (B6) yields the differential equation used in [25],

$$\frac{dM}{dH} = c\frac{dM_{anh}}{dH} + (1 - c)\frac{M_{anh} - M_{irr}}{\delta k - \alpha(M_{anh} - M_{irr})}. \quad (B9)$$

This is equivalent to the formulation used in [14]. For small values of c, from Eq. (5) [equal to Eq. (A5)] it follows that $M \cong M_{irr}$ and, thus, Eq. (B7) approximates Eq. (A2). This means that, with the same parameters set, Eqs. (B9) and (A13) produce very similar hysteresis loops, provided that c is small.

In the work where M_{irr} was first introduced [24], the magnetization was defined as the sum of reversible and irreversible components

$$M = M_{rev} + M_{irr}, \quad (B10)$$

where the reversible magnetization was

$$M_{rev} = c(M_{anh} - M). \quad (B11)$$

Combining Eqs. (B10) and (B11) yields

$$M = \frac{c}{1 + c}M_{anh} + \frac{1}{1 + c}M_{irr}. \quad (B12)$$

Taking the derivative with respect to H and using Eq. (B6) result in the following differential equation reported in that work,

$$\frac{dM}{dH} = \frac{c}{1+c}\frac{dM_{anh}}{dH} + \frac{1}{1+c}\frac{M_{anh} - M_{irr}}{\delta k - \alpha(M_{anh} - M_{irr})}, \quad (B13)$$

Later, from 1989 onwards [14], M was replaced by M_{irr} also in Eq. (B11),

$$M_{rev} = c(M_{anh} - M_{irr}). \quad (B14)$$

Thus, instead of leading to Eq. (B12), this redefinition of the reversible magnetizations yields Eq. (5) [equal to Eq. (A5)], the form that persisted in subsequent versions of the model.

In 1994, Jiles revised the effective field felt by the magnetic moments of the anhysteretic magnetization so that M_{anh} is given by Eq. (4) [22],

$$M_{anh} = M_S \mathcal{L}\left(\frac{H + \alpha M_{anh}}{a}\right). \quad (B15)$$

In the same work, Eq. (B5) was revised to

$$M_{irr} = M_{anh} - \frac{\delta k}{1-c}\frac{dM_{irr}}{dH_{eff}}, \quad (B16)$$

with the only difference of scaling the k parameter by $1/(1-c)$. However, neither Eq. (B15) nor Eq. (B16) persisted in later works by Jiles et al.

REFERENCES

[1] R. C. Smith and C. L. Hom, "Domain wall theory for ferroelectric hysteresis," *Journal of intelligent material systems and structures,* vol. 10, pp. 195-213, 1999. https://doi.org/10.1177/1045389X9901000302

[2] R. S. Stirbu and L. Mitoseriu, "Modeling of hysteretic response of porous piezo/ferroelectric ceramics," *Computational Materials Science,* vol. 232, p. 112633, 2024. https://doi.org/10.1016/j.commatsci.2023.112633

[3] COMSOL_Multiphysics_5.6, "Hysteresis in Ferroelectric Material," 2020 https://doc.comsol.com/5.6/doc/com.comsol.help.models.acdc.ferroelectric_hysteresis/models.acdc.ferroelectric_hysteresis.pdf 01/03/2025

[4] D. H. Wolpert and W. G. Macready, "No free lunch theorems for search," Technical Report SFI-TR-95-02-010, The Santa Fe Institute, 1996

[5] D. H. Wolpert and W. G. Macready, "No free lunch theorems for optimization," *IEEE Transactions on Evolutionary Computation,* vol. 1, pp. 67-82, 1997. https://doi.org/10.1109/4235.585893

[6] Y. C. Ho and D. L. Pepyne, "Simple explanation of the no-free-lunch theorem and its implications," *Journal of Optimization Theory and Applications,* vol. 115, pp. 549-570, 2002. https://doi.org/10.1023/A:1021251113462

[7] J. Ugarte Valdivielso, J. I. Aizpurua Unanue, and M. Barrenetxea Iñarra, "Uncertainty distribution assessment of Jiles-Atherton parameter estimation for inrush current studies," *IEEE Transactions on Power Delivery,* vol. 39, pp. 2275 - 2285, 2024. https://doi.org/10.1109/TPWRD.2024.3398790

[8] K. Chwastek and J. Szczygłowski, "Estimation methods for the Jiles-Atherton model parameters - a review," *Przegląd Elektrotechniczny,* vol. 84, pp. 145-148, 2008 https://api.semanticscholar.org/CorpusID:109039200

[9] D. Jiles and D. Atherton, "Ferromagnetic hysteresis," *IEEE Transactions on Magnetics,* vol. 19, pp. 2183-2185, 1983. https://doi.org/10.1109/TMAG.1983.1062594

[10] S. E. Zirka, Y. I. Moroz, R. G. Harrison, and K. Chwastek, "On physical aspects of the Jiles-Atherton hysteresis models," *Journal of Applied Physics,* vol. 112, 2012. https://doi.org/10.1063/1.4747915

[11] H. Singh and S. D. Sudhoff, "Reconsideration of energy balance in Jiles–Atherton model for accurate prediction of B–H trajectories in ferrites," *IEEE Transactions on Magnetics,* vol. 56, pp. 1-8, 2020. https://doi.org/10.1109/TMAG.2020.2994022

[12] Y. Ma, E. Wang, H. Yang, and S. Yao, "Reconsideration of nonphysical solution in Jiles–Atherton model for real-time hysteresis estimation," *IEEE Transactions on Magnetics,* vol. 58, pp. 1-9, 2022. https://doi.org/10.1109/TMAG.2022.3163891

[13] J. Chen, H. Shang, D. Xia, S. Wang, T. Peng, and C. Zang, "A modified vector Jiles-Atherton hysteresis model for the design of hysteresis devices," *IEEE Transactions on Energy Conversion,* vol. 38, pp. 1827-1835, 2023

[14] D. C. Jiles and J. Thoelke, "Theory of ferromagnetic hysteresis: Determination of model parameters from experimental hysteresis loops," *IEEE Transactions on Magnetics,* vol. 25, pp. 3928-3930, 1989. https://doi.org/10.1109/20.42480

[15] P. Weiss, "L'hypothèse du champ moléculaire et la propriété ferromagnétique," *J. Phys. Theor. Appl.,* vol. 6, pp. 661-690, 1907. https://doi.org/10.1051/jphystap:019070060066100

[16] J. D. van der Waals, "Over de Continuiteit van den Gas- en Vloeistoftoestand (The continuity of the liquid and gaseous states of matter, translated by R. Threlfall and J. F. Adair, Physical memoirs selected and translated from foreign sources under the direction of the Physical Society of London, Vol 1, Part 3, Taylor and Francis, London, 1890), University of Leiden," 1873 https://books.google.com.ar/books?id=1A1jAAAAcAAJ (English version: https://catalog.hathitrust.org/Record/008905142)

[17] D. Jiles, *Introduction to magnetism and magnetic materials*: CRC press, 2015. https://doi.org/10.1201/b18948

[18] D. C. Jiles and D. L. Atherton, "Theory of ferromagnetic hysteresis (invited)," *Journal of Applied Physics,* vol. 55, pp. 2115-2120, 1984. https://doi.org/10.1063/1.333582

[19] J. M. Silveyra and J. M. C. Garrido, "On the modelling of the anhysteretic magnetization of homogeneous soft magnetic materials," *Journal of Magnetism and Magnetic Materials,* vol. 540, p. 168430, 2021. https://doi.org/10.1016/j.jmmm.2021.168430

[20] J. M. Silveyra and J. M. Conde Garrido, "A physically based model for soft magnets' anhysteretic curve," *JOM,* vol. 75, pp. 1810-1823, 2023. https://doi.org/10.1007/s11837-023-05704-x

[21] D. C. Jiles and Y. Melikhov, "Modelling of nonlinear behaviour and hysteresis in magnetic materials," *Handbook of Magnetism and Advanced Magnetic Materials,* p. 15, 2007. https://doi.org/10.1002/9780470022184.hmm223

[22] D. C. Jiles, "Frequency dependence of hysteresis curves in conducting magnetic materials," *Journal of Applied Physics,* vol. 76, pp. 5849-5855, 1994. https://doi.org/10.1063/1.358399

[23] D. Jiles and D. Atherton, "Theory of the magnetisation process in ferromagnets and its application to the magnetomechanical effect," *Journal of Physics D: Applied Physics,* vol. 17, p. 1265, 1984. https://doi.org/10.1088/0022-3727/17/6/023

[24] D. C. Jiles and D. L. Atherton, "Theory of ferromagnetic hysteresis," *Journal of Magnetism and Magnetic Materials,* vol. 61, pp. 48-60, 1986. https://doi.org/10.1016/0304-8853(86)90066-1

[25] D. C. Jiles, J. Thoelke, and M. Devine, "Numerical determination of hysteresis parameters for the modeling of magnetic properties using the theory of ferromagnetic hysteresis," *IEEE Transactions on Magnetics,* vol. 28, pp. 27-35, 1992. https://doi.org/10.1109/20.119813

[26] J. P. A. Bastos and N. Sadowski, *Electromagnetic modeling by finite element methods*: CRC press, 2003. https://doi.org/10.1201/9780203911174

[27] R. Szewczyk, "Computational problems connected with Jiles-Atherton model of magnetic hysteresis," *Recent Advances in Automation, Robotics and Measuring Techniques. Advances in Intelligent Systems and Computing,* vol. 267, pp. 275-283, 2014. https://doi.org/10.1007/978-3-319-05353-0_27

[28] A. Benabou, S. Clenet, and F. Piriou, "Comparison of Preisach and Jiles–Atherton models to take into account hysteresis phenomenon for finite element analysis," *Journal of Magnetism and Magnetic Materials,* vol. 261, pp. 139-160, 2003. https://doi.org/10.1016/S0304-8853(02)01463-4

[29] Matlab. *ode23tb - Solve stiff differential equations — trapezoidal rule + backward differentiation formula*. Available: https://www.mathworks.com/help/matlab/ref/ode23tb.html. Access date: 31/03/2025

[30] M. Hosea and L. Shampine, "Analysis and implementation of TR-BDF2," *Applied Numerical Mathematics,* vol. 20, pp. 21-37, 1996. https://doi.org/10.1016/0168-9274(95)00115-8

[31] D. A. Philips, L. R. Dupre, and J. A. Melkebeek, "Comparison of Jiles and Preisach hysteresis models in magnetodynamics," *IEEE Transactions on Magnetics,* vol. 31, pp. 3551-3553, 1995. https://doi.org/10.1109/20.489566

[32] D. Lederer, H. Igarashi, A. Kost, and T. Honma, "On the parameter identification and application of the Jiles-Atherton hysteresis model for numerical modelling of measured characteristics," *IEEE Transactions on Magnetics,* vol. 35, pp. 1211-1214, 1999. https://doi.org/10.1109/20.767167

[33] K. Chwastek and J. Szczygłowski, "An alternative method to estimate the parameters of Jiles–Atherton model," *Journal of Magnetism and Magnetic Materials,* vol. 314, pp. 47-51, 2007. https://doi.org/10.1016/j.jmmm.2007.02.157

[34] H. Wu, G. Xue, H. Bai, and Z. Ren, "A new modeling methodology for frequency-dependent hysteresis from the perspective of phase lag and amplitude attenuation," *Nonlinear Dynamics,* vol. 113, pp. 7759–7777, 2024. https://doi.org/10.1007/s11071-024-10531-z

[35] S. C. Chapra, *Applied numerical methods with MATLAB for engineers and scientists*, 5th edition ed.: McGraw-Hill, 2023

[36] M. Toman, G. Stumberger, and D. Dolinar, "Parameter identification of the Jiles–Atherton hysteresis model using differential evolution," *IEEE Transactions on Magnetics,* vol. 44, pp. 1098-1101, 2008. https://doi.org/10.1109/TMAG.2007.915947

[37] L. dos Santos Coelho, V. C. Mariani, and J. V. Leite, "Solution of Jiles–Atherton vector hysteresis parameters estimation by modified Differential Evolution approaches," *Expert Systems with Applications,* vol. 39, pp. 2021-2025, 2012. https://doi.org/10.1016/j.eswa.2011.08.035

[38] R. Biedrzycki, R. Szewczyk, P. Švec, and W. Winiarski, "Determination of Jiles-Atherton model parameters using differential evolution," *Mechatronics - Ideas for Industrial Application. Advances in Intelligent Systems and Computing,* vol. 317, pp. 11-18, 2015. https://doi.org/10.1007/978-3-319-10990-9_2

[39] R. Szewczyk, "Two step, differential evolution-based identification of parameters of Jiles-Atherton model of magnetic hysteresis loops," *Automation 2018. Advances in Intelligent Systems and Computing,* vol. 743, pp. 635-641, 2018. https://doi.org/10.1007/978-3-319-77179-3_60

[40] X. Ju, J. Lu, B. Rong, and H. Jin, "Parameter identification of displacement model for giant magnetostrictive actuator using differential evolution algorithm," *Actuators,* vol. 12, p. 76, 2023. https://doi.org/10.3390/act12020076

[41] A. Regan, J. Wilson, and A. J. Peyton, "Extension to the Jiles–Atherton hysteresis model using Gaussian distributed parameters for quenched and tempered engineering steels," *Sensors,* vol. 25, p. 1328, 2025. https://doi.org/10.3390/s25051328

[42] K. Chwastek and J. Szczyglowski, "Identification of a hysteresis model parameters with genetic algorithms," *Mathematics and Computers in Simulation,* vol. 71, pp. 206-211, 2006. https://doi.org/10.1016/j.matcom.2006.01.002

[43] V. Khemani, M. H. Azarian, and M. G. Pecht, "Efficient identification of Jiles–Atherton model parameters using space-filling designs and genetic algorithms," *Eng,* vol. 3, pp. 364-372, 2022. https://doi.org/10.3390/eng3030026

[44] L. d. S. Coelho, F. A. Guerra, and J. V. Leite, "Multiobjective exponential particle swarm optimization approach applied to hysteresis parameters estimation," *IEEE Transactions on Magnetics,* vol. 48, pp. 283-286, 2012. https://doi.org/10.1109/TMAG.2011.2172581

[45] Y.-Q. Guo, M. Li, Y. Yang, Z.-D. Xu, and W.-H. Xie, "A particle-swarm-optimization-algorithm-improved Jiles–Atherton model for magnetorheological dampers considering magnetic hysteresis characteristics," *Information,* vol. 15, p. 101, 2024. https://doi.org/10.3390/info15020101

[46] B. Bai, J. Wang, and K. Zhu, "Identification of the Jiles-Atherton model parameters using simulated annealing method," *2011 International Conference on Electrical Machines and Systems,* pp. 1-4, 2011. https://doi.org/10.1109/ICEMS.2011.6073612

[47] R. A. Naghizadeh, B. Vahidi, and S. Hossein Hosseinian, "Parameter identification of Jiles-Atherton model using SFLA," *COMPEL-The International Journal for Computation and Mathematics in Electrical and Electronic Engineering,* vol. 31, pp. 1293-1309, 2012. https://doi.org/10.1108/03321641211227573

[48] M. Zou, "Parameter estimation of extended Jiles–Atherton hysteresis model based on ISFLA," *IET Electric Power Applications,* vol. 14, pp. 212-219, 2020. https://doi.org/10.1049/iet-epa.2019.0384

[49] Z. Chen, Y. Yu, and Y. Wang, "Parameter identification of jiles-atherton model based on levy whale optimization algorithm," *IEEE Access,* vol. 10, pp. 66711-66721, 2022. https://doi.org/10.1109/ACCESS.2022.3185414

[50] M. Trapanese, "Identification of parameters of the Jiles–Atherton model by neural networks," *Journal of Applied Physics,* vol. 109, 2011. https://doi.org/10.1063/1.3569735

[51] A. Schäfer, Y. Gong, and N. Parspour, "Fast identification of the Jiles-Atherton-model parameters and the electric conductivity based on Gaussian process regression," *IEEE Transactions on Magnetics,* 2025. https://doi.org/10.1109/TMAG.2025.3541244

[52] A. Schäfer, S. Weigel, and N. Parspour, "Efficient and versatile anhysteretic magnetization models for soft magnetic materials in FEA and Circuit simulations," *IEEE Transactions on Magnetics,* 2025. https://doi.org/10.1109/TMAG.2025.3539352

[53] J. Pearson, P. Squire, and D. Atkinson, "Which anhysteretic magnetization curve?," *IEEE Transactions on Magnetics,* vol. 33, pp. 3970-3972, 1997. https://doi.org/10.1109/20.619632

[54] J. M. Silveyra, M. I. González, T. F. González, and J. M. C. Garrido, "MagAnalyst: A MATLAB toolbox for anhysteretic magnetization analysis," *IEEE Transactions on Magnetics,* vol. 60, 2024. https://doi.org/10.1109/TMAG.2024.3408681

[55] J. M. Silveyra and J. M. Conde Garrido, "On the anhysteretic magnetization of soft magnetic materials," *AIP Advances,* vol. 12, 2022. https://doi.org/10.1063/9.0000328

[56] J. Pytlík, J. Luňáček, and O. Životský, "Differential isotropic model of ferromagnetic hysteresis," *Physical Review B,* vol. 108, p. 104414, 2023. https://doi.org/10.1103/PhysRevB.108.104414

[57] K. Chwastek, P. Gębara, A. Przybył, R. Gozdur, A. P. Baghel, and B. S. Ram, "An alternative formulation of the harrison model," *Applied Sciences,* vol. 13, p. 12009, 2023. https://doi.org/10.3390/app132112009

[58] R. Oldenhuis. *minimize - Minimize constrained functions with FMINSEARCH or FMINLBFGS, globally or locally*. Available: https://www.mathworks.com/matlabcentral/fileexchange/24298-minimize, https://github.com/rodyo/FEX-minimize/releases/tag/v1.8. Access date: 03/11/2023

[59] J. D'Errico. *interparc - Distance based interpolation along a general curve in space*. Available: https://www.mathworks.com/matlabcentral/fileexchange/34874-interparc. Access date: 31/03/2025

[60] O. Bottauscio, M. Chiampi, C. Ragusa, L. Rege, and M. Repetto, "Description of TEAM Problem: 32 - A test case for validation of magnetic field analysis with vector hysteresis," *IEEE Transactions on Magnetics,* vol. 38, pp. 893-896, 2002. https://doi.org/10.1109/20.996230

[61] K. Hoffmann, J. P. A. Bastos, J. V. Leite, N. Sadowski, and F. Barbosa, "A vector Jiles–Atherton model for improving the FEM convergence," *IEEE Transactions on Magnetics,* vol. 53, pp. 1-4, 2017. https://doi.org/10.1109/TMAG.2017.2660303

[62] R. Szewczyk, "Jiles–Atherton model for Octave/MATLAB," 2021 https://www.github.com/romanszewczyk/JAmodel/ 01-01-2021

[63] M. Ohta and Y. Yoshizawa, "Recent progress in high Bs Fe-based nanocrystalline soft magnetic alloys," *Journal of Physics D: Applied Physics,* vol. 44, p. 064004, 2011. https://doi.org/10.1088/0022-3727/44/6/064004

[64] G. Xue, C. Zhang, H. Bai, X. Ren, and Z. Ren, "An improvement of the Jiles-Atherton model at various magnetic field amplitudes using the example of Terfenol-D material," *Journal of Magnetism and Magnetic Materials,* vol. 601, p. 172172, 2024. https://doi.org/10.1016/j.jmmm.2024.172172

[65] N. Sadowski, N. Batistela, J. Bastos, and M. Lajoie-Mazenc, "An inverse Jiles-Atherton model to take into account hysteresis in time-stepping finite-element calculations," *IEEE Transactions on Magnetics,* vol. 38, pp. 797-800, 2002. https://doi.org/10.1109/20.996206

[66] J. H. Deane, "Modeling the dynamics of nonlinear inductor circuits," *IEEE Transactions on Magnetics,* vol. 30, pp. 2795-2801, 1994. https://doi.org/10.1109/20.312521

[67] M. Hamimid, M. Feliachi, and S. Mimoune, "Modified Jiles–Atherton model and parameters identification using false position method," *Physica B: Condensed Matter,* vol. 405, pp. 1947-1950, 2010. https://doi.org/10.1016/j.physb.2010.01.078

[68] A. Raghunathan, Y. Melikhov, J. E. Snyder, and D. Jiles, "Theoretical model of temperature dependence of hysteresis based on mean field theory," *IEEE Transactions on Magnetics,* vol. 46, pp. 1507-1510, 2010. https://doi.org/10.1109/TMAG.2010.2045351

[69] D. C. Jiles, "A self consistent generalized model for the calculation of minor loop excursions in the theory of hysteresis," *IEEE Transactions on Magnetics,* vol. 28, pp. 2602-2604, 1992. https://doi.org/10.1109/20.179570

[70] D. Jiles, A. Ramesh, Y. Shi, and X. Fang, "Application of the anisotropic extension of the theory of hysteresis to the magnetization curves of crystalline and textured magnetic materials," *IEEE Transactions on Magnetics,* vol. 33, pp. 3961-3963, 1997. https://doi.org/10.1109/20.619629

[71] D. Jiles, X. Fang, and W. Zhang, *Modeling of hysteresis in magnetic materials. In: Liu, Y., Sellmyer, D.J., Shindo, D. (eds) Handbook of Advanced magnetic materials. Springer, Boston, MA.*: Springer, 2006. https://doi.org/10.1007/1-4020-7984-2_17

[72] F. Liorzou, B. Phelps, and D. Atherton, "Macroscopic models of magnetization," *IEEE Transactions on Magnetics,* vol. 36, pp. 418-428, 2000. https://doi.org/10.1109/20.825802

[73] W. M. Kiarie, E. J. Barron, A. Baghel, I. Nlebedim, M. D. Bartlett, and D. C. Jiles, "Modeling of magnetic properties of magnetorheological elastomers using JA hysteresis model," *IEEE Transactions on Magnetics,* vol. 57, pp. 1-5, 2020. https://doi.org/10.1109/TMAG.2020.3024878

[74] D. C. Jiles and W. Kiarie, "An integrated model of magnetic hysteresis, the magnetomechanical effect, and the Barkhausen effect," *IEEE Transactions on Magnetics,* vol. 57, pp. 1-11, 2020. https://doi.org/10.1109/TMAG.2020.3034208